

## Low energy charged particles in near Martian space from the SLED and LET experiments aboard the Phobos-2 spacecraft

V.V. Afonin<sup>1</sup>, S.M.P. McKenna-Lawlor<sup>2</sup>, G. Erdos<sup>3</sup>, K.I. Gringauz<sup>1</sup>, E. Keppler<sup>4</sup>, K. Kecskemety<sup>3</sup>, E. Kirsch<sup>4</sup>, R.G. Marsden<sup>5</sup>, A.K. Richter<sup>4</sup>, W. Riedler<sup>6</sup>, K. Schwingenschuh<sup>6</sup>, A. Somogyi<sup>3</sup>, D. O'Sullivan<sup>7</sup>, L. Szabo<sup>3</sup>, A. Thompson<sup>7</sup>, A. Varga<sup>3</sup>, K-P Wenzel<sup>5</sup>, M. Witte<sup>4</sup>, Ye Yeroshenko<sup>8</sup>, L. Zeleny<sup>1</sup>

1. Space Research Institute, Moscow, USSR
2. Space Technology Ireland, St. Patrick's College, Maynooth, Ireland.
3. Central Research Institute for Physics, Budapest, Hungary
4. Max Planck Institut fuer Aeronomie, Lindau, West Germany
5. Space Science Department of ESA, ESTEC Noordwijk, The Netherlands
6. Institut fuer Weltraumforschung, Graz, Austria
7. Dublin Institute for Advanced Studies, Ireland
8. Institute of Terrestrial Magnetism, Ionosphere and Radio Wave Propagation, Troitsk, Moscow Region, USSR

(Camera-ready copy received in final form 6 September 1990)

### ABSTRACT

*The charged particle detector SLED on the Phobos-2 spacecraft has recorded, during a number of circular orbits about Mars, significant fluxes of ions with energies up to 200 keV in close spatial association with the Martian bow shock. The observed characteristics of these enhancements suggest that different shock acceleration mechanisms were operative in producing individual events*

### 1. Introduction

The charged particle detector SLED aboard the three-axis stabilized Phobos-2 spacecraft, was designed to measure, simultaneously, fluxes of ions and electrons in the 30 keV to a few MeV range, McKenna-Lawlor et al. 1990. The instrument used silicon surface barrier detectors, two in each of two telescopes which viewed in the same direction. One telescope (Te 2) was covered by a thin Al-foil ( $500 \mu\text{g}\cdot\text{cm}^{-2}$  Al. on mylar) whereas the other telescope (Te 1) was open. The front detectors of both telescopes were covered by a  $15 \mu\text{g}\cdot\text{cm}^{-2}$  Al. layer.

Low energy protons and electrons could be distinguished since Te 2 stopped ions (protons) up to 350 keV, due to its Al-foil and the Al-layer mounted on the front detector. The geometric factor of each telescope was  $0.21 \text{ cm}^2 \text{ ster}$  and the field of view (FOV) axis, with a  $40^\circ$  apex angle, was in the ecliptic plane at  $55^\circ$  to the sunward direction (that is in the nominal direction of the interplanetary magnetic field at Mars).

Anticoincidence signals from the back detectors were used to reject particles which penetrated the front detectors. In addition, each telescope was shielded by  $5.6 \mu\text{g}\cdot\text{cm}^{-2}$  Al and Ta, to prevent protons with energies  $> 70 \text{ MeV}$  and

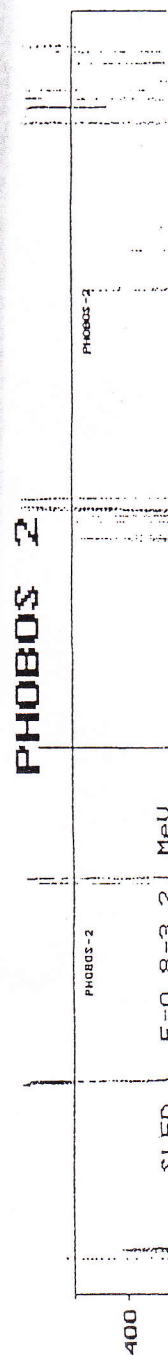
electrons with energies  $> 10$  MeV from reaching the detector systems. Thus, six different energy channels for each telescope could be realized. In the open telescope (Te 1), ions and electrons were recorded in the following, approximate, ranges; Ch. 1 (30-50 keV); Ch. 2 (50-200 keV); Ch. 3 (200-600 keV); Ch. 4 (0.6-3.2 MeV); Ch. 5 (3.2-4.5 MeV); Ch. 6 ( $> 30$  MeV). In the foil covered "electron" telescope Te 2, the energy ranges covered by individual channels were closely similar to the above. Channel 6 in both telescopes provided the count rates of the back detectors. In Te 2, protons with energies  $< 350$  keV; He ions  $< 1.6$  MeV and oxygen ions  $< 8$  MeV were stopped in the Al-layers. SLED was the first instrument with the capability to measure particles of energies  $> 30$  keV to approach Mars as closely as 867 km.

The LET instrument comprised a solid state detector telescope designed to detect low energy cosmic ray nuclei in the range 1 to 75 keV/n, with species resolution extending from hydrogen up to iron, Marsden *et al.* 1990. Count rate information was available for protons in 5 energy channels; for alpha particles in 4 channels; for heavy ions in 7 channels and for electrons in 1 channel. Pulseheight analysis (PHA) data was also provided. In order to obtain coarse anisotropic measurements, the LET sensor was mounted on a scanning platform whose angular range of  $175^\circ$  was divided into four equal steps. The scan plane lay approximately in the ecliptic and the extreme viewing directions were chosen to coincide with the orientation of the average interplanetary magnetic field at the orbit of Mars.

SLED and LET together measured charged particles over a range that extended from approximately 30 keV to several tens of MeV/n. The time resolution of SLED was 4 minutes and that of LET between 4 and 20 minutes. In both instruments, particle fluxes and energy distribution spectra were measured. In the case of LET, chemical composition and flux anisotropy measurements were also made. Both instruments operated successfully throughout the Phobos-2 mission. Fig. 1 provides an overview of the fluxes recorded by both instruments in selected energy channels. It is noted that the Phobos-2 Cruise Phase was very rich in the incidence of energetic solar particle events of different types. Not all of these events can be recognized in Fig. 1, which is presented using a linear scale. Rather, Fig. 1 highlights a number of very intense events which define the most active time intervals to occur during the mission.

In addition to the data obtained during the Cruise Phase, data from 5 elliptical orbits executed by the spacecraft when close to Mars and, afterwards, in 114 circular orbits at a height above the planet's surface of about 6900 km, are available (the latter period of revolution was  $08^h 04^m$ ). In these circular orbits, the instruments recorded a number of different effects which require detailed analysis. This report deals with one of these effects, namely energetic ion flux increases in the energy range 30-200 keV, recorded by SLED along certain lengths, close to the bow shock, of the circular orbits.

Before presenting these results, it is useful to recall that previous measurements of high energy charged particles in the near Martian environment were made in 1972 by the Soviet spacecraft Mars-2, Vernov *et al.* 1974. However, the lowest



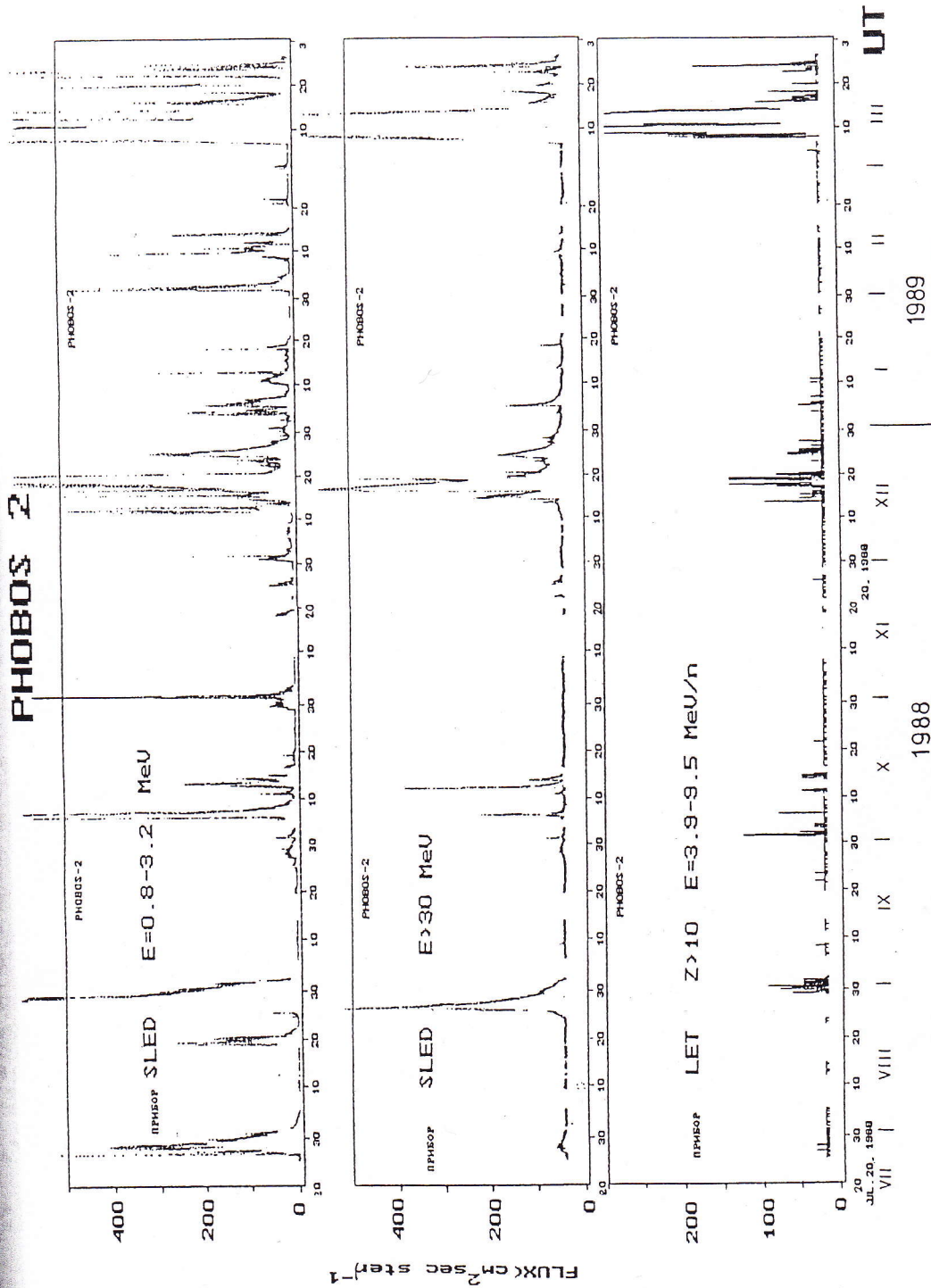


Fig.1; Fluxes of energetic ions in selected energy channels recorded by SLED (top two panels) and by LET (bottom panel) on Phobos-2 during the working lifetime of the spacecraft

energy thresholds of the onboard particle experiment were, in this case, 100 keV for electrons and 1 MeV for protons.

## 2. Observations

In certain of the circular orbits, significant count rate increases in the low energy channels were sometimes recorded by the SLED instrument. These increases occurred only in 'open' telescope Te 1. No enhancement was correspondingly observed in the foil protected telescope so that the increases recorded in Te 1 seem to have been produced by energetic ions. Fig. 2 shows several examples of such events; data from the four lowest energy channels of SLED are presented. The first event illustrated (top panel) was observed at about 08<sup>h</sup> U.T. and the second a little after 15<sup>h</sup> U.T. on 17 March 1989. On this day, the spacecraft was spinning around its, sun directed, X-axis (period of spin, about 11.8<sup>m</sup>). The amplitudes of the particle increases recorded were 1-1.5 orders of magnitude and they each comprised sequences of smooth and relatively wide (1.5<sup>h</sup>) peaks, returning periodically to the background level. As the field of view of the SLED aperture was relatively small (40° full cone), the latter modulation can be interpreted to be due to the spin of the spacecraft. Figure 2 also shows that count rate increases were recorded only in the energy range ~30-200 keV. Similar phenomena were identified on other days, for example, on 23 February, 1989 (see the lower panel).

The count rate increases displayed in Fig.2 were recorded approximately at the terminator region on both sides of the planet. It should be noted that, according to data obtained by the Phobos-2 onboard magnetic field and plasma instruments, the planetary bow shock was also located in this region. The observed count rate increases may be interpreted to be due to charged particle flux enhancements associated with the bow shock. Alternatively, they might be a consequence of sunlight scattered into the instrument from the planet (the front detector of Te 1 was only shielded by 15  $\mu\text{g cm}^{-2}$  Al., so that this detector was potentially sensitive to sunlight).

Initially, the possibility that sunlight reflected from the body of the planet (rather than from its thin atmosphere) had entered the aperture of the instrument was investigated. To implement this, the field of view screening of SLED by the planet body was calculated, taking into account the real spacecraft orbit and the attitude of the instrument aperture. These calculations show that, during the whole period when circular orbits were made, the field of view of the SLED aperture was crossed by the planet while the spacecraft was moving along its trajectory - maximum field of view coverage about 50%. Reflected sunlight could enter the aperture only at one side of the planet under spin stabilized conditions. During those orbits when the spacecraft was spinning, light contamination could occur on both sides.

If light penetration into the aperture was responsible for the enhancements recorded, then we would expect to see such events regularly, with a periodicity of about 8 hours, in the same segment of each orbit. The data presented in Fig.2b however show no such periodicities in the count rates and, from these

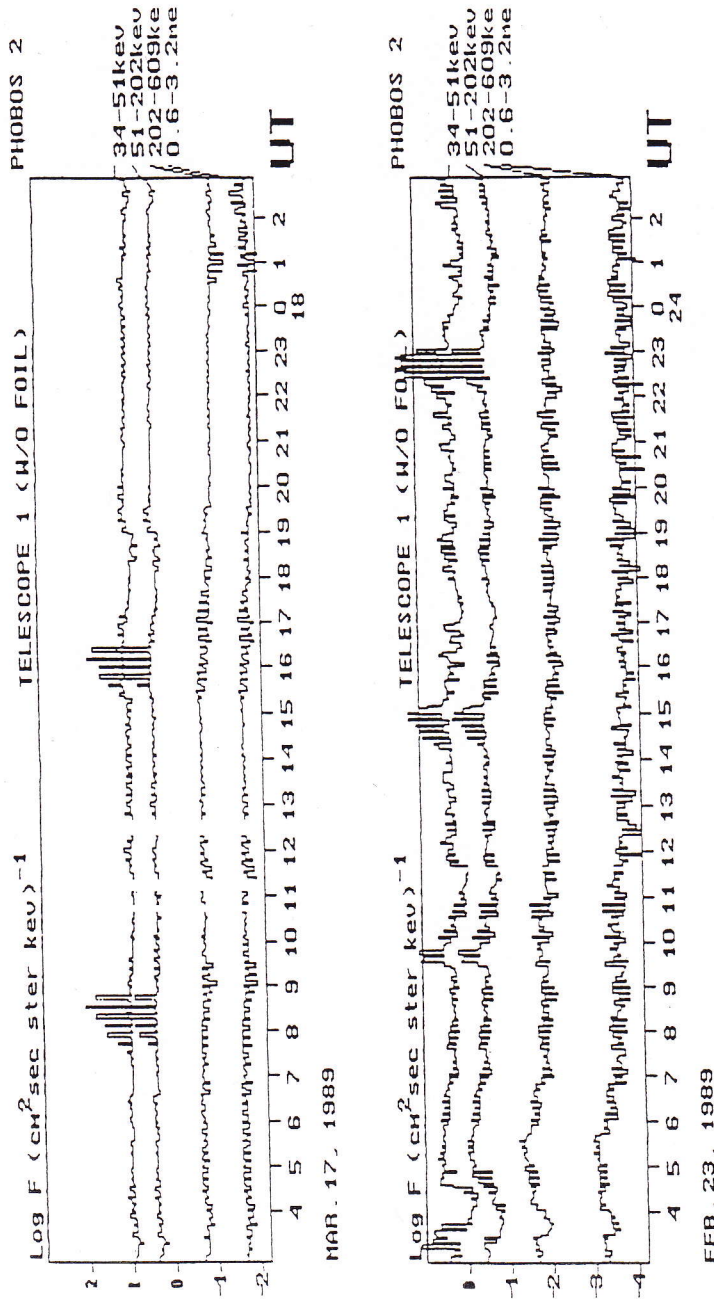


Fig. 2; Examples of count rate increases relative to background, recorded by SLED in Te 1 during selected circular orbits. No corresponding enhancements were observed in the foil protected telescope.

and other data not presented here, it follows that the flux enhancements recorded did not occur on a periodic basis. During the greater part of the observations, no special flux enhancements were recorded at all. Furthermore, calculation shows that the photon fluxes reflected from Mars can hardly contribute to the observed count rates of approximately  $10^3$  counts per second, McKenna-Lawlor *et al.* 1990. Hence, we may conclude that the recorded count rate increases are due to 'real' ion fluxes.

An additional indication in favour of the above interpretation is that the increases recorded were always observed just before, or just after, the bow shock (as defined by the magnetic field data). In many cases, a very narrow peak was observed just at the bow shock. In certain, rare, cases, similar enhancements were recorded deep inside the 'night' magnetosphere.

### 3. Results from a Preliminary Analysis

Two aspects of the observed particle enhancements have been considered here, namely (a) their location along the orbit trajectory relative to the main features of the magnetosphere and (b) properties of the energy spectra of these fluxes.

Firstly, the positions of the flux enhancements along the orbit were correlated with magnetic field data obtained, simultaneously, on Phobos-2 by the onboard magnetometer. Secondly, the energy distribution spectra were calculated (all spectral calculations were made without averaging, so that the time resolution concerned is 4m).

Representative results are shown in Figs. 3-5. All of these figures are composed similarly and consist of several panels. Starting at the top, the two upper panels show, respectively, the sun-spacecraft component of the magnetic field,  $B_x$  and the magnetic field magnitude  $B$ . The next panel displays, using a linear

---

Fig.3; Simultaneous energetic ion and magnetic field measurements made aboard Phobos-2 during Circular Orbit 87 on 17 March, 1989. Two top panels; Sun-spacecraft line component of the magnetic field  $B_x$  and the magnetic field magnitude  $B$ . Three central panels; measured fluxes of energetic ions recorded by Te 1 in the lowest energy channel of SLED (34-51 keV): calculated shadowing of the SLED aperture field of view in relative units (non spinning spacecraft); spectral index determined, with a time resolution of 4m, through fitting a power law to the first four steps of each spectrum. Bottom left; two spectra; one for background counts, labeled B; one for the peak of the flux increases. The shaded area is the difference between the peak spectrum and the background spectrum. Bottom right; various parameters, represented by lines drawn perpendicular to points along four mutually displaced contours representing a particular orbit. These parameters are (starting from the inside), the measured particle fluxes in Te 1, Ch. 1; the magnetic field component  $B_x$ ; the direction of the magnetic field vector in the ecliptic plane; the magnitude of the magnetic field  $B$ . The sun is at the left side.

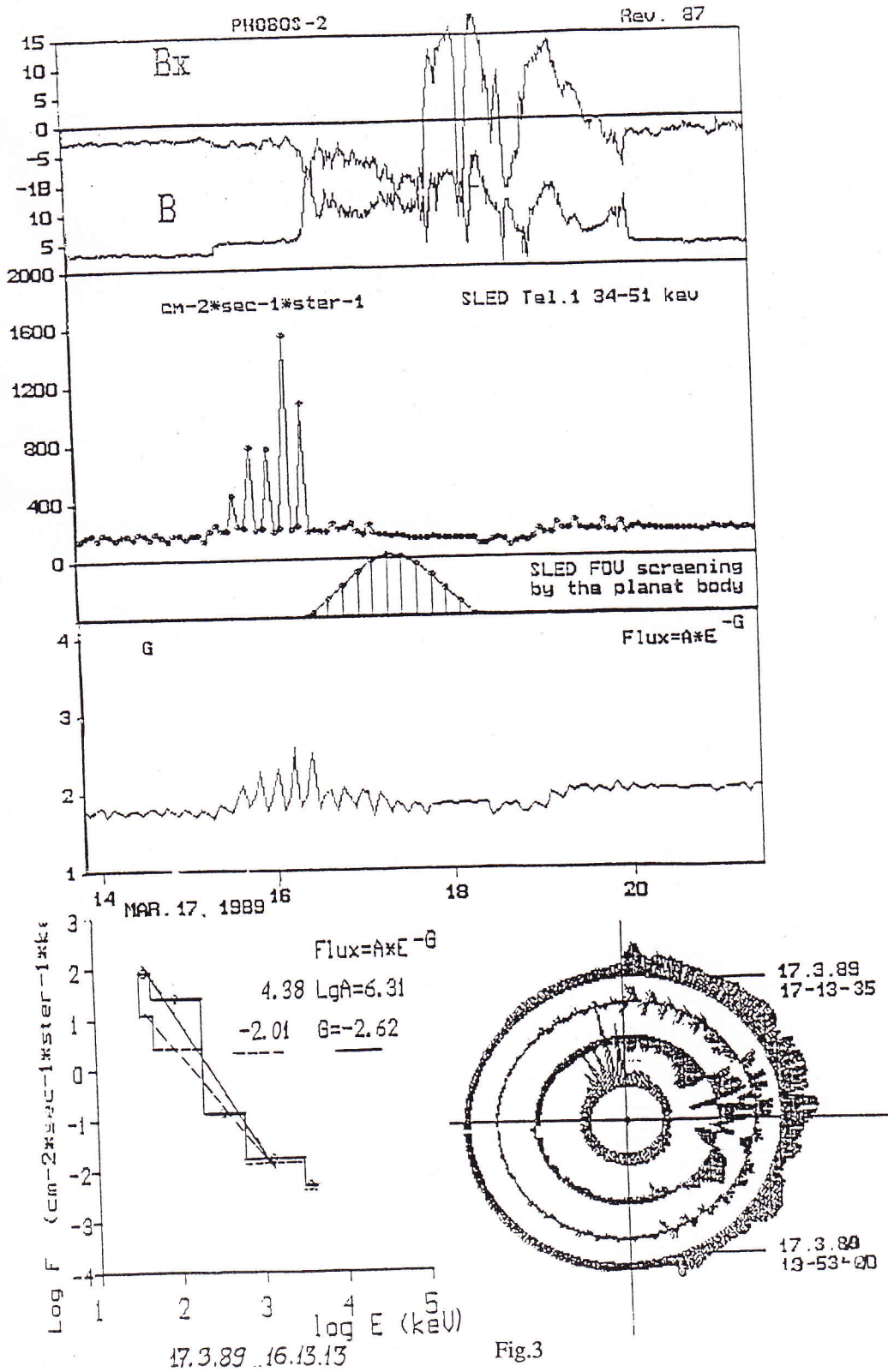


Fig.3

scale, the measured fluxes of energetic ions for the lowest energy channel of the SLED instrument ( $\sim 30-50$  keV). Fig. 5 provides, in addition, data from the second energy channel ( $\sim 50-200$  keV). Next, is presented the calculated shadowing of the SLED aperture field of view in relative units (presuming a non spinning spacecraft).

The last panel shows the spectral index, measured and calculated every 4m. To get the spectral index, the first four steps of each spectrum were fitted by a power law  $F = A * E^{-G}$  (using a least square fitting technique), where A represents amplitude and G the spectral index. The lower left inset shows two spectra; one refers to the background, labeled 'B', the other is for the peak of the flux increases. Background spectra were calculated both outside and inside the region of flux increase, just immediately before the flux peaked due to spacecraft spin. In all cases, the background spectra were observed to be very stable, thus implying that strongly anisotropic fluxes were detected. The shaded area is the difference between the peak spectrum and the background spectrum.

The lower right inset shows a number of significant parameters drawn on a set of nested contours, each representing the same circular orbit. For each parameter, the orbit trajectory is shown scaled up, with the value of the parameter concerned represented by a line, drawn perpendicular to that part of the orbit path where it was measured. The lengths of perpendicular lines are drawn to be proportional to particular parameter values. These parameters comprise, starting from the inside

- Measured charged particle fluxes
- $B_x$ , the spacecraft-sun component of the magnetic field B
- The direction of the magnetic field vector in the ecliptic plane
- The magnitude of the magnetic field B

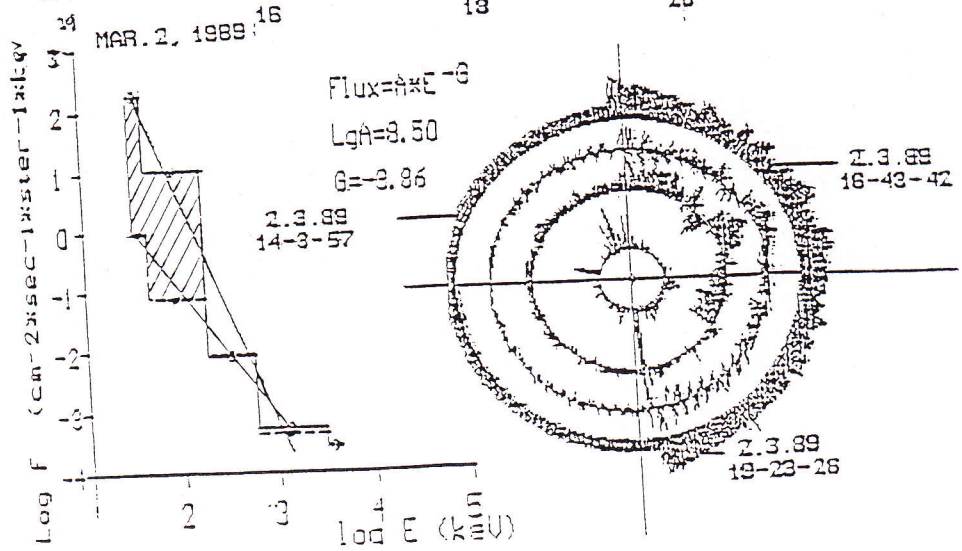
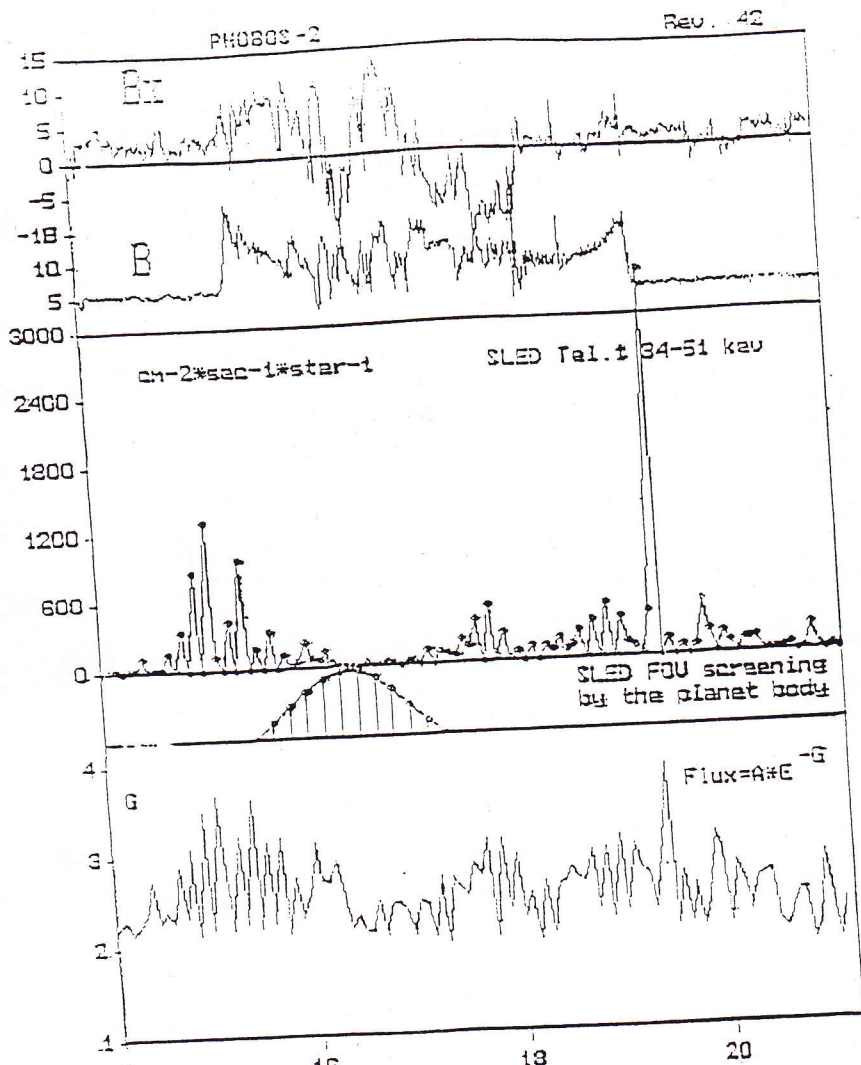
The sun is at the left side of the drawing.

In each of the Figures 3-5, the position of the bow shock is clearly defined by an abrupt increase in the magnitude of B. In Fig.3 (Circular Revolution 87), can be seen the preshock region, together with the position of the bow shock; the increase of  $B_x$  inside the magnetosphere; the magnetospheric lobes (characterized by a sunward and antisunward  $B_x$  component) and, in the plasmashet region, numerous reversals of the  $B_x$  direction.

Particle flux enhancements were, in general, found to occur in a broad region within the undisturbed interplanetary medium, just before the spacecraft crossed the bow shock on entering the Martian magnetosphere. Similar flux increases were also often observed in the undisturbed interplanetary medium, just after the crossing of the bow shock as the spacecraft exited the magnetosphere. The form of the maximum, in these cases, was the same as in the typical case illustrated in Fig. 3. Sometimes the maximum comprised a very narrow peak of width  $d \ll p_1$ , (where  $p_1$  represents the ion gyroradius). As a rule, the

---

Fig.4; The same as in Fig. 4 but for 02 March, 1989 (Circular Rev. 42)



02.03.89 19.2545 Fig.4

amplitude of such narrow peaks was much higher than that recorded in the case of a broad ( $d = p_1$ ) maximum. Fig. 4 illustrates a 'broad maximum' flux event recorded by SLED at the spacecraft entered the magnetosphere as well as a very narrow, and much more intense, peak recorded at it exited. The figure additionally shows that, deep inside the magnetosphere, several minor flux increases occurred. Such events were observed relatively rarely and their amplitude was always much less than the amplitude of those enhancements recorded near the bow shock region.

On 27 February, 1989 (Circular Revolution 34), the spacecraft was 3-axis stabilized and Fig. 5 shows a flux increase observed just after the spacecraft crossed the bow shock at the entrance to the magnetosphere (i.e. when the spacecraft was in the magnetosheath). The width of the peak was, again  $d = p_1$  but the form of the event suggests the presence of two (or more) superimposed maxima, the first one wide and smooth, with  $d = p_1 = \sim 10000$  km and the other(s) narrow and more intense. In this figure, data from the second SLED energy channel (50-200 keV) are also presented. It is seen that, in this latter energy range, the flux increases were much smaller than in the 30-50 keV range.

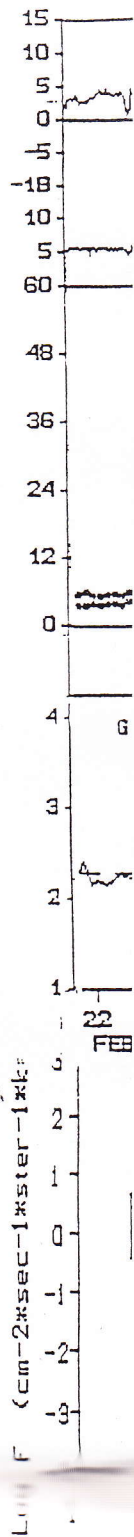
The time behaviour of the spectral index  $G$  indicates that the slopes of the spectra recorded inside the observed maxima were much higher than was the case for spectra recorded outside the maxima. The background spectra were found to display remarkable stability both outside and inside the region of the flux increases (see the spectra as well as the slope  $G$  time profiles provided in Figs. 3-5 for three representative events). Inside the enhanced region, the background spectra could be observed due to spacecraft spin modulation. The data set suggests that the spacecraft crossed, during these events, strongly directed fluxes of energetic particles.

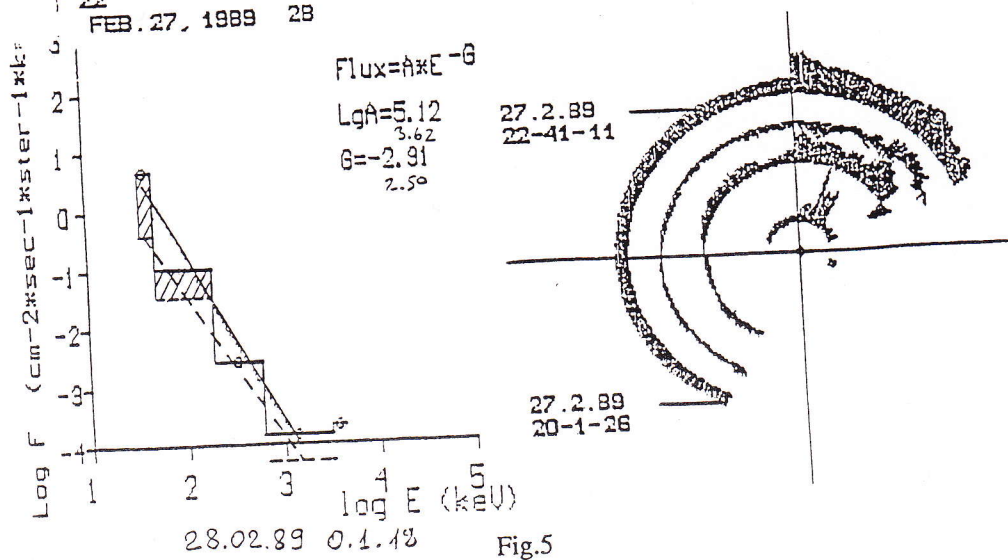
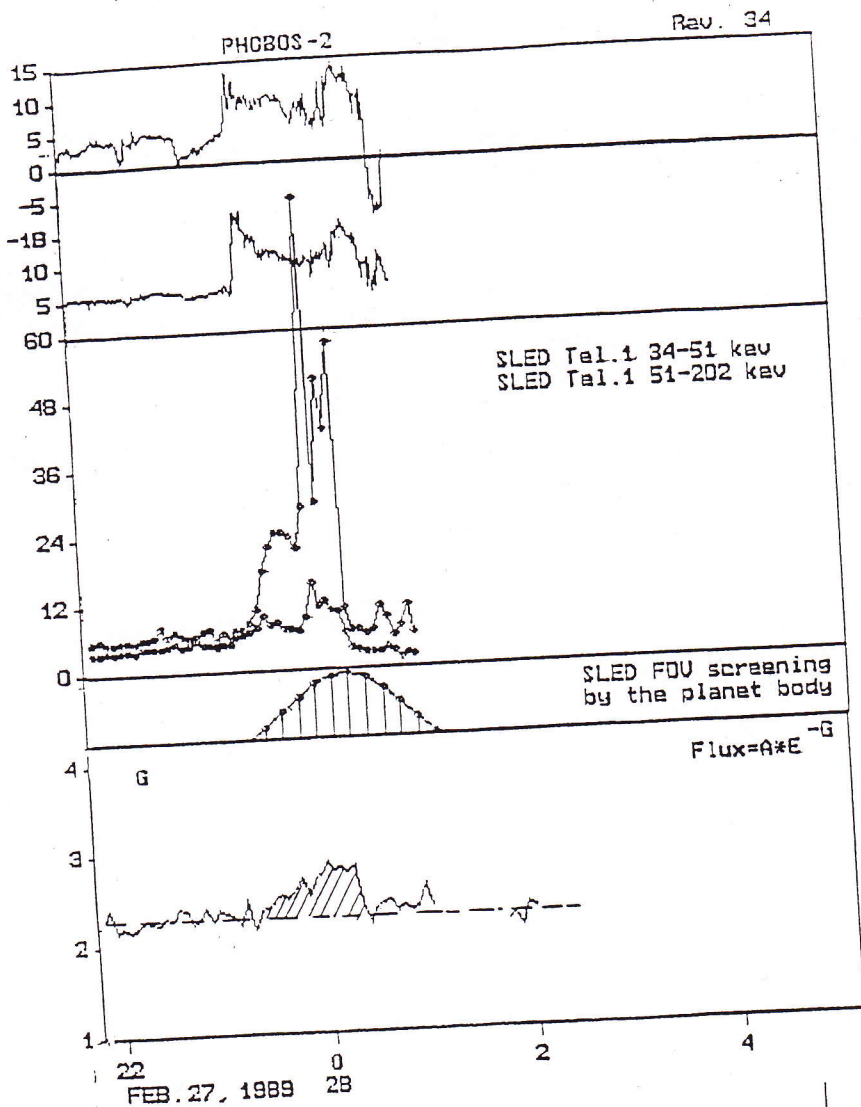
Taking into account the absence of spin modulated effects outside the region of flux enhancement, as well as the characteristics of the background spectra both inside and outside the regime of flux increase, one may conclude that Phobos-2 crossed jets of energetic particles embedded into the, practically, uniform and isotropic energetic particle medium. These jets were well pronounced and strongly anisotropic. They consisted of energetic ions with energies up to 200 keV.

In summary the following phenomena were observed;

1. Large ion flux increases, up to 1.5 orders of magnitude ( $E = 30-200$  keV), in a broad region of width  $d = p_1$ , upstream, and sometimes downstream, of the bow shock in the magnetosheath region of the Martian magnetosphere. In both upstream and downstream situations, the flux increases recorded occurred adjacent to the bow shock.

Fig.5; The same as in Fig. 5 but for 27-28 February, 1989 (Circular Rev. 34). The spacecraft, at this time, was in its 3-axis stabilized mode.





2. Intense narrow spikes of width  $d \ll p_1$  exactly at the bow shock.
3. Similar, but less intense, flux increases, deep inside the Martian magnetosphere (relatively rare).

The various flux increases recorded were strongly anisotropic.

#### 4. Discussion

To interpret the observations it is necessary to discover the reason for the observed flux increases. To this end, it is necessary to make detailed comparisons of the particle observations with other data sets to find out (a) the shock geometry; (b) the seed population available for acceleration; (c) the SLED aperture altitude relative to the ambient magnetic field; (e) the kinds of wave fields present. Such detailed comparisons can only be made when "de-spun" magnetic field data become available to provide necessary insights into the shock structure.

Without these data, we may suggest that the observed flux increases were due to bow shock acceleration. The observed two different patterns of large flux increases seem to relate to the two major shock acceleration mechanisms.

It is well known that bow shock acceleration has already been observed in association with the Earth's bow shock and with various interplanetary shocks. Usually, two bow shock acceleration mechanisms are invoked, namely drift and diffusive acceleration mechanisms. The first is most effective in the case of quasi-perpendicular or perpendicular shocks ( $\theta_{VB} = 45^\circ\text{-}90^\circ$ ). The second is relevant to the case of quasi-longitudinal, or longitudinal shocks ( $\theta_{VB} = 0^\circ\text{-}45^\circ$ ), where  $\theta_{VB}$  is the angle between the shock normal and the mean upstream magnetic field.

For the diffusive acceleration mechanism to be effective, the presence of electromagnetic fluctuations is necessary. In this connection it is interesting that the magnetic field measured by the onboard MAGMA instrument became turbulent before the bow shock, as observed during the elliptical orbits, and showed large variations in direction during the circular orbits, Riedler *et al.* 1989. Figs. 3-5 show only the magnitude ( $B$ ), and one component of the magnetic field. These data display relatively small magnetic fluctuations before the bow shock and much higher fluctuations after the spacecraft had crossed this feature. Changes in the magnetic field direction (not shown in Figs. 3-5), were always present, both before and after the bow shock, and these features were of relatively large magnitude.

The Plasma Wave System (PWS) instrument aboard the Phobos-2 spacecraft recorded electron plasma oscillations upstream of the Martian bow shock, Gard *et al.* 1990. The downstream magnetosheath was characterized by broadband electric field noise below the plasma frequency. In the shock foot, the broad

band noise extended from below the lower hybrid frequency to the electron plasma frequency.

The narrow flux spikes recorded by SLED just at the bow shock, see for example Figure.4, appear to have been due to drift acceleration at the shock. As the peak illustrated includes only two points (i.e. 8 minute coverage), the corresponding shock thickness was approximately 1000 km, which is much less than the energetic ion gyroradius. SLED could directly observe ions accelerated along the shock surface as its aperture field of view, in each spacecraft spin, viewed along the bow shock surface.

Another possible explanation may be invoked in association with heavy pick-up ions. During the second Phobos-2 orbit around Mars, and prior to crossing the bow shock, the experiment ASPERA measured intense ( $> 1.5$  orders of magnitude) increases in the  $O^+$  ion density, as well as in the densities of the heavier ion group ( $CO_2^+$ ,  $CO^+$  and  $CO_2^+$ ). There was, simultaneously, a drop in the density of  $H^+$  ions, Lundin et al. 1989.

The lowest energy channel of SLED responds, in the case of protons, to  $\sim 30$ -50 keV of energy deposited in the solid-state detector by an incoming particle. In the case of heavier ions, due to the pulse-height defect in silicon detectors, the deposited energies are less than the primary energies of incoming particles, Keppler, 1978. Preflight calibration of a similar detector by  $M = 18$  ( $H_2O^+$ ) ions showed that this channel of SLED responds to water group ions with energies of approximately 100 keV, McKenna-Lawlor et al. 1985. In the spacecraft frame of reference, a freshly picked up oxygen ion could attain such an energy if the velocity of the solar wind were  $500 \text{ kms}^{-1}$  (assuming that the ambient magnetic field and the solar wind velocity are mutually perpendicular).

Of course the observed flux increases can be explained in this way if, at the height of the spacecraft above Mars (approximately 6000 km), there are enough seed neutral oxygen atoms. Due to the small scale height of the Martian atmosphere, atmospheric oxygen and heavier atoms cannot reach this altitude in sufficient numbers. Hot atmospheric oxygen atoms could however reach the height of the spacecraft orbit. According to Nagy et al., 1989 the main source of hot oxygen ions is from the dissociative recombination of  $O_2^+$  ions. The excess energy of oxygen atoms in this reaction lies in the range 0.8-0.96 eV. Modeling by Nagy et al. 1989 of the hot oxygen density  $n(O)$  height profile for solar minimum conditions has shown this profile to be essentially flat, with  $n(o) = 10^2 \text{ cm}^{-3}$  at 3000 km altitude. If we accept this value, then the corresponding estimate for a height of 6000 km (assuming an  $r^{-2}$  radial dependence), yields a value of  $n(O)$  approximately equal to  $10^1 \text{ cm}^{-3}$ . With an appropriate direction of the interplanetary magnetic field, such a density could produce the observed energetic particle flux increases. As the gyroradius of such ions is  $> 3$ -4  $R_m$  (where  $R_m = \text{Martian radius}$ ) the increases recorded could only be produced in conditions when a favorable magnetic field direction was present. It is unlikely that the observed features of the ion flux increases can be explained by the pick up process.

## 5. Conclusion

The energetic particle detectors aboard the Phobos-2 spacecraft have shown that, at the Martian bow shock, acceleration of ambient ions up to an energy of 200 keV occurs. The observed characteristics of the particle signatures have their origin in different shock acceleration mechanisms.

## References

1. McKenna-Lawlor, S.M.P., Afonin, V.V., Gringauz, K., Keppler, E., Kirsch, E., Richter, A.K., Witte, M., O'Sullivan, D., Thompson, A., Somogyi, A., Szabo, L. and Varga, A. "The low energy particle detector SLED ( $\sim 30$  keV-3.2 MeV) and its performance on the Phobos Mission to Mars and its moons " (1990) Nuclear Inst. and Methods. in Phys. Res. A290, 217
2. Marsden, R.G., Afonin, V.V., Balazs, A., Erdos, G., Henrion, J.P.G., Richter, A.K., Rusznyak, P., Somogyi, A., Szalai, S., Varga, A., Varhalmi, L., Wenzel, K-P, and Witte, M. (1990) Nuclear Inst. and Methods. in Phys. Res. A290, 211
3. Vernov, S.N., Tverskoi, B.A., Yakovlev V.A., Gorchakov, E.V., Ignatiev, P.P., Liubimov, G.P., Marchenko, O.A., Shvidkovskaia, T.E., Kontor, N.N., Morozova, T.I., Nikolaev, A.G., Rosental, I.A., Chiuchkov, E.A., Getzelev, I.V., Onishenko, L.V. and Tkachenko, V. I. (1974) Potokizar jashenix chastits v okrestnosti Marsa ( Charged Particle fluxes in the Mars environment), Kosmich Issled XII, No.2, 252
4. Riedler, W., Mohlmann, D., Oraevsky, V.N., Schwingenschuh, K., Yeroshenko, Ye, Rustenback, J., Aydogar, Oe, Berghofer, G., Lichtenegger, H., Delva, M., Schelch, G., Pirsch, K., Fremuth, G., Steller, M., Arnold, H., Radtach, T., Auster, U., Fornacon, K.H., Schenk, H.J., Michaelis, H., Motschmann, U., Roatasch, T., Sauer, K., Schroter, R., Kurths, J., Lenners, D., Linthe, J., Kobzev, V., Styashkin, V., Achache, J., Slavin, J., Luhmann, J.G. and Russell, C.T. (1990), Magnetic fields near Mars; first results, Nature, 341, 604
5. Grard, R., Pedersen, A., Klimov, S. Savin, S., Skalsky, A., Trotignon, J.G. and Kennel, C. (1990) First measurements of plasma waves near Mars, Nature, 341, 607
6. Lundin, R., Zakharov, A., Pellinen, R., Borg, H., Hultqvist, B., Pissarenko, N., Dubinin, E.M., Barabash, S.W., Liede, I. and Koskinen H. (1990) First measurements of the ionospheric plasma escape from Mars, Nature 341, 609
7. Keppler, E. (1978) A note on the complications of the Compton-Getting effect for low energy charged particle measurements in interplanetary space Geophys. Res. Lett., 5, No. 1, 69.
8. McKenna-Lawlor, S., Kirsch, E. Thompson, A., O'Sullivan D. and Wenzel K.-P.(1985) Energetic particles in the comet Halley environment Adv. Space Res., 1, No. 12, 211
9. Nagy, A.F. and Cravens, T.E. (1989) Hot oxygen atoms in the upper

A CON

**ABSTRACT**  
interaction w  
discussed bri  
of magnetic f  
with a dipole  
involving cap  
field lines fro  
discovered in

## 1. INTRO

Surprisingly e  
data yet obt  
understanding  
from earlier r  
presently unde  
improvement  
secure in our k  
as, for exampl  
The most stri  
total of the p  
characteristics  
with correctio  
are potentially  
the ionosphere  
ions which are  
Two and perh  
atmosphere is  
outer boundar  
is made evider  
disappearance  
and possibly a